Evaluation for Overall Volume of Capacitor and Heat-sink in Step-down Rectifier using Modular Multilevel Converter

Toshiki Nakanishi and Jun-ichi Itoh
Nagaoka University of Technology
1603-1 Kamitomioka-cho,
Nagaoka city Niigata, Japan
Tel. / Fax: +81/ (258) – 47 – 9533.
E-Mail: nakanishi@stn.nagaokaut.ac.jp, itoh@vos.nagaokaut.ac.jp
URL: http://itohserver01.nagaokaut.ac.jp/itohlab/index.html

Keywords

«Modular Multilevel Converter», «H-bridge cell», «High power density design», «Step-down rectifier»

Abstract

This paper discusses a volume evaluation of a step-down rectifier using a Modular Multilevel Converter (MMC) for a power system connected to a utility gird of 6.6 kV in order to obtain the high power density. Specifically, this paper evaluates a relationship among an output voltage of the MMC, a volume of capacitors and a volume of a heat-sink. At first, formulas of semiconductor losses are clarified. Second, the relationship between the ripple current and the volume of electrolytic capacitors is considered. In addition, the relationship between the number of cells per leg and an overall volume is also shown. According to these considerations, the evaluation result of the overall volume shows that it is necessary to reduce a step-down ratio of the MMC in order to obtain the high power density. Moreover, it is also necessary to approach a withstand voltage ratio to 1.0 when the withstand voltage ratio is defined as the ratio of the required withstand voltage to an actual withstand voltage with series connection capacitors. In conclusion, the volume of the proposed system becomes approximately 20% of the volume of a conventional power system of 200 kVA connected to the utility gird of 6.6 kV.

I. Introduction

Recently, a micro-grid and a DC power grid have been actively researched as next generation power supplies [1]-[2]. Specifically, the DC micro-grid is suitable to connect a battery energy storage system and a renewable energy source such as a photovoltaic generation system or a fuel cell to the DC grid because the output voltages of many renewable energy sources are DC [1]-[2]. From this feature, the DC micro-grid is expected as a new generation power grid system.

The DC micro-grid is connected to an AC power grid of 6.6 kV as one of power sources. Moreover, transformers are applied between the AC power grid and the DC micro-grid in order to step-down 6.6 kV into several hundred volts and obtain isolation between the AC power grid and the DC micro-grid. However, a volume of the isolated transformer increases because the isolated transformer operates in a commercial frequency. In addition, a conventional power system connected to the utility gird of 6.6 kV also includes static capacitors in order to correct an input power factor and a series reactor in order to reduce a harmonic distortion of a grid current. Thus, the volume of the conventional power system connected to the utility gird increases.

As one of solutions, the employment of Modular Multilevel Converter (MMC) to the power system connected to the DC micro-grid is an effective method. The MMC has been actively researched as a next generation high power converter without the bulky transformer [3]-[4]. Therefore, the power system connected to the utility gird in the DC micro-grid achieves the volume reduction by applying the MMC into the system. Additionally, the MMC achieves a step-down rectification by replacing a chopper cell into an H-bridge cell because the H-bridge cell has no limitation in the offset of an output

voltage of the cell compared to the chopper cell [4]-[5]. The MMC achieves the reduction of static capacitors and the series reactor because the MMC controls the input power factor and reduce the harmonic distortion. Thus, the step-down rectifier using the MMC achieves the reduction of the system volume.

On the other hand, in terms of the realization of the high power density in the step-down rectifier using the MMC, it is necessary to consider the design method in order to reduce the volume of a capacitor with a high capacity and a heat-sink on each H-bridge cell. So far, an evaluation of the capacitor volume has been reported in terms of the capacitance and the electrostatic energy [6]. Moreover, in terms of the design for the heat-sink, a calculation method of semiconductor losses, analysis of semiconductor losses in simulations and a transition of the semiconductor loss when the input power factor changes have been also reported [7]-[10]. In addition, the design criteria for the volume minimization of an electrolytic capacitor on each cell in terms of a ripple current have been considered because the ripple current affects a lifetime of the electrolytic capacitor [5]. However, it seems that an overall volume which is combined the capacitor volume and the heat-sink volume has not been considered. Moreover, the proposed system also includes an isolated DC-DC converter in later part of the MMC. Thus, the system divides step-down functions at the MMC and the DC-DC converter. Therefore, the step-down ratio of the MMC should be decided in order to obtain the high power density.

In this paper, the clarification of the design criteria in order to achieve the high power density in the step-down rectifier using the MMC is detailed. Specifically, each fundamental evaluation for the volume of capacitors and the volume of the heat-sink is considered respectively. The conditions in order to achieve the volume reduction are clarified by the relationship and the characteristic which are found from fundamental evaluations even in the case which the circuit parameters of the MMC changes complexly. At first, the clarification of semiconductor losses in the H-bridge cell is reported. Second, the relationship between the output voltage of the MMC and the overall volume which is combined the volume of capacitors and the volume of the heat-sink is considered. Additionally, the relationship between the number of cells per leg and overall volume is also shown. Finally, conditions in order to obtain the high power density are clarified from the each relationship.

II. System configuration

2.1. Conventional power system connected to utility grid

Figure 1 shows a structure of the conventional power system of 200 kVA connected to the utility gird [11]. The conventional system has several transformers in order to convert from the grid voltage of 6.6 kV into the AC distribution voltage of 200 V or 100 V. Moreover, the system also includes static capacitors in order to correct the input power factor and the series reactor in order to reduce a harmonic distortion of the grid current. Thus, the volume of the conventional power system increases.

2.2. Proposed system

Figure 2 shows the main circuit configuration of the proposed step-down rectifier using the MMC. Each leg consists of two buffer reactors L_b and the H-bridge cells. The converter outputs a multi-level voltage waveform in order to reduce harmonic distortions of the input current. Thus, many cascaded cells are used in practical because the reduction effect of the harmonic distortion increases by increasing the number of cells. Additionally, the MMC is able to reduce the voltage rating of devices on each cell because of cascade connections of cells. Therefore, lower voltage rating devices are utilized to the MMC. On the other hand, the output DC voltage of the MMC depends on the sum of the cell's output average voltage. Thus, the output voltage of the cell includes the AC component and the DC component in order to control the input current and the output voltage. Moreover, the MMC converts the high AC voltage to the DC voltage of several hundreds volts. After this step, the DC voltage of 400 V is supplied to the DC bus of the DC distribution by the isolated DC-DC converter. Thus, the input side and the output side are isolated by the DC-DC converter.

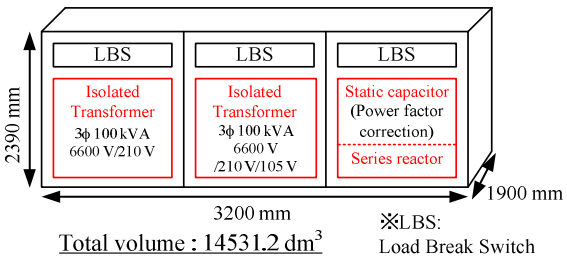

Fig. 1. Conventional power system of 200 kVA connected to utility gird of 6.6 kV

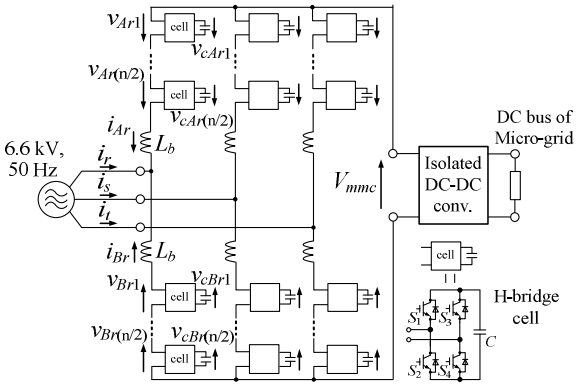

Fig. 2. Circuit configuration of step-down rectifier using MMC.

Ⅲ. Control strategy

3.1. Concept of proposed control for the MMC

Figure 3 shows a control block diagram of the proposed step-down converter [5]. The proposed control system is based on the single-phase power factor correction (PFC) converter because the H-bridge cell has same circuit configuration as singe-phase PFC converter. Differences between the PFC converters and the H-bridge cells are; there is a DC component in the output voltage of the H-bridge cell, and a voltage balancing control is necessary in order to correct unbalance voltages among all capacitors. Thus, in order to deal with above problems, it is necessary to add two control systems to control the DC component and achieve the voltage balancing.

3.2. Average voltage control

The average voltage control is applied in order to control the average value of all capacitor voltage in the arm [5]. Therefore, the average value of all capacitor voltages has to be calculated in each arm. In addition, the error between the voltage command and the average value of all capacitor voltages in the arm is corrected by a PI controller. The output value of the PI controller is given as the positive phase component's command of the arm current. Moreover, the voltage command v_C^* is given by (1).

$$v_C^* \geq \frac{1}{n\lambda}\left(2\sqrt{\frac{2}{3}}E + V_{mmc}\right) \tag{1}$$

where E is an effective value of the input line-to-line voltage. V_{mmc} is the output DC voltage of the MMC. n is the number of cells at each leg. Note that the modulation index λ is set to 0.8 in this paper.

3.3. Arm current control

Each arm current includes the AC component and the DC component. First, the AC component of the arm current flows from the power grid. The AC component is defined as a positive phase component. Moreover, from the previous section, the positive phase component's command is generated by the average voltage control. In other words, the AC component of the arm current is controlled in order to maintain the average value of all capacitor voltages in each arm constant.

On the other hand, the arm current also includes the DC component (a zero phase component). Therefore, it is necessary to eliminate only the zero phase component from the arm current in order to control the capacitor voltage. In this paper, the application of the rotational coordinate transform is applied. This method extracts the positive phase component by using the rotational coordinate transform in each arm group; the upper side and the lower side.

3.4. Output voltage control

The output DC power is controlled by the zero phase component. The command of the output DC voltage is added into the output value of the controller in the arm current control. Moreover, the output

DC voltage of the MMC is divided on each cell. Thus, the output DC voltage of one cell is fundamentally set as V_{mmc}^{*}/n when the command of the MMC output voltage control is V_{mmc}^{*}.

3.5. Voltage balancing control

The voltage balancing control corrects the unbalance voltage which occurs among capacitors in same arm. In the proposed voltage balancing control, the output DC voltage of the cell is varied depending on the capacitor voltage [6]. The biggest advantage of the proposed voltage balancing control system is that it is not necessary to design control parameters because the dividing ratio is adjusted automatically depending on the capacitor voltage.

IV. Clarification of semiconductor losses on H-bridge cell

In this section, formulas of semiconductor losses on the H-bridge cell are clarified for the design of the heat-sink. At first, it is necessary to analyze the arm current which flows to each switching device because the arm current significantly changes when the input power factor changes. Second, formulas of semiconductor losses are clarified based on the result of arm current analysis.

4.1. Analysis of arm current

At first, the cell output voltage and the arm current are defined by (2) and (3) respectively in lower side of the MMC. The cell output voltage and the arm current have the DC component and the AC component.

$$v_{B\_cell} = \frac{1}{n}\left\{2\sqrt{\frac{2}{3}}E\cos(\theta+\phi)+V_{mmc}\right\} \tag{2}$$

$$i_{Br} = -\frac{1}{2}\sqrt{\frac{2}{3}}\frac{S}{E}\cos\theta+\frac{P}{3V_{mmc}} \tag{3}$$

where S is an input apparent power. ϕ is the input phase difference.

From (3), the condition which the arm current becomes the DC is given by (4).

$$\frac{P}{3V_{mmc}} \geq \frac{1}{2}\sqrt{\frac{2}{3}}\frac{S}{E} \tag{4}$$

Moreover, the condition which the current includes only the DC component is given by (5).

$$\frac{2}{3}\sqrt{\frac{3}{2}}\frac{E}{V_{mmc}}\cos\phi-1 \geq 0 \tag{5}$$

Additionally, an angle θ_0 which a direction of the arm current changes is defined by (6) when the arm current is AC.

$$\theta_0 = \cos^{-1}\left(\frac{2}{3}\sqrt{\frac{3}{2}}\frac{E}{V_{mmc}}\cos\phi\right) \tag{6}$$

From (6), the section θ_a which the positive current flows against the definitional direction of the arm current is given by (7). In contract, the section θ_b which the negative current flows is given by (8).

$$-\pi \leq \theta_a \leq -\theta_0, \quad \theta_0 \leq \theta_a \leq \pi \tag{7}$$

$$-\theta_0 \leq \theta_b \leq \theta_0 \tag{8}$$

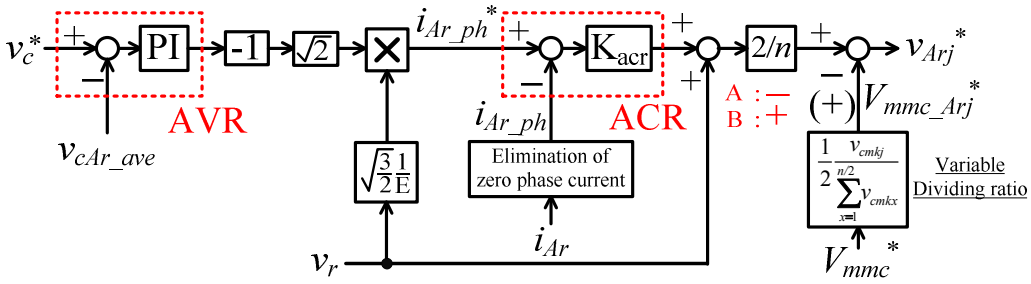

Fig.3. Control block diagram for one arm of MMC.

Figure 4 shows the relationship among the cell output voltage, the arm current and θ_a and θ_b.

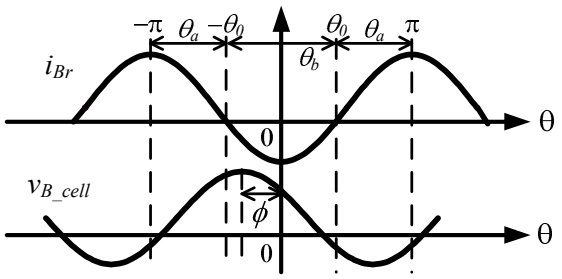

Fig.4. Relationship between cell output voltage and arm current in lower side of MMC.

4.2. Calculation of conduction loss

In the system, the general PWM modulation is applied. Thus, S_1 and S_4 which is shown in Fig. 2 operate in pairs. In contract, S_2 and S_3 operate in pairs. Thus, the semiconductor losses are same in pair devices. Therefore, in this paper, only semiconductor losses of one leg in the H-bridge cell are calculated.

The average value of the conduction loss at one cycle P_{con} is given by (9) [12].

$$P_{con} = \frac{1}{2\pi}\int_{\alpha}^{\beta}\left(V_0 + Ri_{B\_cell}\right) i_{B\_cell} d_{SD}\ d\theta \tag{9}$$

where V_0 is a voltage drop when the current is zero. R is a resistance value of the device. Both values are calculated from the datasheet of the device. i_{B_cell} is the current which flows to the device. d_{SD} is the duty of each switching device.

The current which flows to S_1, S_4, D_2 and D_3 when the arm current becomes the positive is given by (10). In contract, the current which flows to S_2, S_3, D_1 and D_4 when the arm current is negative is given by (11). Note that the variable number θ of (10) is replaced θ_a and θ of (11) is replaced θ_b.

$$i_{B\_cell\_P} = -\frac{1}{2}\sqrt{\frac{2}{3}}\frac{S}{E}\cos\theta_a + \frac{P}{3V_{mmc}} \tag{10}$$

$$i_{B\_cell\_N} = \frac{1}{2}\sqrt{\frac{2}{3}}\frac{S}{E}\cos\theta_b - \frac{P}{3V_{mmc}} \tag{11}$$

Moreover, each duty is given by (12), (13), (14) and (15).

$$d_{S1} = \frac{1}{2}\left\{1 + \frac{1}{nV_C}\left(2\sqrt{\frac{2}{3}}E\cos\left(\theta_a + \phi\right) + V_{mmc}\right)\right\} \tag{12}$$

$$d_{S2} = \frac{1}{2}\left\{1 - \frac{1}{nV_C}\left(2\sqrt{\frac{2}{3}}E\cos\left(\theta_b + \phi\right) + V_{mmc}\right)\right\} \tag{13}$$

$$d_{D1} = 1 - d_{S2} \tag{14}$$

$$d_{D2} = 1 - d_{S1} \tag{15}$$

where V_C is the capacitor voltage.

Each conduction loss of S_1 and S_2 is given by (16) and (17) respectively. Note that formulas of conduction losses on D_1 and D_2 are omitted because each formula is complex.

$$\begin{aligned}
P_{B_S1_Con} = {} & \frac{V_{0_SW}}{4\pi}\left[\left(1+\frac{V_{mmc}}{nV_C}\right)\left\{\sqrt{\frac{2}{3}}\frac{S}{E}\sin\theta_0 + \frac{2}{3}\frac{P}{V_{mmc}}\left(\pi-\theta_0\right)\right\} + \frac{1}{nV_C}\left\{-\frac{P}{3}\left(2\left(\pi-\theta_0\right)-\sin 2\theta_0\right) - \frac{4}{3}\sqrt{\frac{2}{3}}\frac{PE}{V_{mmc}}\cos\phi\sin\theta_0\right\}\right] \\
& + \frac{R_{SW}}{4\pi}\left[\left(1+\frac{V_{mmc}}{nV_C}\right)\left\{\frac{1}{12}\frac{S^2}{E^2}\left(2\left(\pi-\theta_0\right)-\sin 2\theta_0\right) + \frac{2}{3}\sqrt{\frac{2}{3}}\frac{PS}{EV_{mmc}}\sin\theta_0 + \frac{2}{9}\frac{P^2}{V_{mmc}^{\ 2}}\left(\pi-\theta_0\right)\right\}\right. \\
& \left. + \frac{1}{nV_C}\left\{-\frac{1}{6}\sqrt{\frac{2}{3}}\frac{PS}{E}\left(3\sin\theta_0 + \frac{1}{3}\sin 3\theta_0\right) - \frac{4}{9}\frac{P^2}{V_{mmc}}\left(\left(\pi-\theta_0\right) - \frac{1}{2}\sin 2\theta_0\right) - \frac{4}{9}\sqrt{\frac{2}{3}}\frac{P^2E}{V_{mmc}^{\ 2}}\cos\phi\sin\theta_0\right\}\right]
\end{aligned} \tag{16}$$

$$P_{B\_S2\_Con}=\frac{V_{0\_SW}}{4\pi}\left[\left(1-\frac{V_{mmc}}{nV_C}\right)\left\{\sqrt{\frac{2}{3}}\frac{S}{E}\sin\theta_0-\frac{2}{3}\frac{P}{V_{mmc}}\theta_0\right\}-\frac{1}{nV_C}\left\{\frac{P}{3}(2\theta_0+\sin 2\theta_0)-\frac{4}{3}\sqrt{\frac{2}{3}}\frac{PE}{V_{mmc}}\cos\phi\sin\theta_0\right\}\right]$$
$$+\frac{R_{SW}}{4\pi}\left[\left(1-\frac{V_{mmc}}{nV_C}\right)\left\{\frac{1}{12}\frac{S^2}{E^2}(2\theta_0+\sin 2\theta_0)-\frac{2}{3}\sqrt{\frac{2}{3}}\frac{PS}{EV_{mmc}}\sin\theta_0\right.\right. \tag{17}$$
$$\left.\left.+\frac{2}{9}\frac{P^2}{V_{mmc}{}^2}\theta_0\right\}-\frac{1}{nV_C}\left\{\frac{1}{6}\sqrt{\frac{2}{3}}\frac{PS}{E}\left(3\sin\theta_0+\frac{1}{3}\sin 3\theta_0\right)-\frac{4}{9}\frac{P^2}{V_{mmc}}\left(\theta_0+\frac{1}{2}\sin 2\theta_0\right)+\frac{4}{9}\sqrt{\frac{2}{3}}\frac{P^2E}{V_{mmc}{}^2}\cos\phi\sin\theta_0\right\}\right]$$

4.3. Calculation of switching loss

The switching loss P_{sw} and the recovery loss P_{Rec} are given by (18) [12].

$$P_{Sw(Rec)}=V_C\frac{1}{2\pi}\int_\alpha^\beta i_B\,d\theta\frac{w}{V_{dcd}I_{md}}f_c \tag{18}$$

where w is each loss energy which is described in the datasheet. V_{dcd} and I_{md} are the voltage value and the current value when w is measured. f_c is the carrier frequency.

Each switching loss on S_1 and S_2 is given by (19) and (20) respectively. Note that formulas of recovery losses on D_1 and D_2 are omitted as with the conduction loss.

$$P_{B\_S1\_SW}=\frac{V_C}{\pi}\left\{-\frac{1}{2}\sqrt{\frac{2}{3}}\frac{S}{E}\sin\theta_0+\frac{P}{3V_{mmc}}\theta_0\right\}\frac{w_{on}+w_{off}}{V_{dcd}I_{md}}f_c \tag{19}$$

$$P_{B\_S2\_SW}=\frac{V_C}{\pi}\left\{-\frac{1}{2}\sqrt{\frac{2}{3}}\frac{S}{E}\sin\theta_0-\frac{P}{3V_{mmc}}(\pi-\theta_0)\right\}\frac{w_{on}+w_{off}}{V_{dcd}I_{md}}f_c \tag{20}$$

V. Experimental results

In this section, experimental results by the miniature model of the MMC are shown. In the experiment, a utility power source of 200 V is applied as the input voltage source.

Figure 5 shows waveforms of the input phase voltage, the input current and the output DC voltage. Firstly, from the waveforms of the input phase voltage and the input current, it is confirmed that the unity power factor is obtained in the input side. Moreover, the total harmonic distortion (THD) of the input current is 5.6%. Second, the waveform of the output DC voltage in lower side of Figure 5 shows that the miniature model converts from the input voltage of 200 V into the output DC voltage of 65 V. From this result, it is confirmed that the output voltage is kept constant. Therefore, the miniature model of the MMC achieves the step-down rectification.

Figure 6 shows the waveforms of cell capacitor voltages which are connected to the r-phase leg. The cell capacitor voltage is controlled according to the capacitor voltage command. As a result, the proposed system maintains the capacitor voltage of each H-bridge cell to the voltage command of 120 V. In addition, the maximum voltage error between the voltage command of the cell capacitor and the measured voltage is 5% or less.

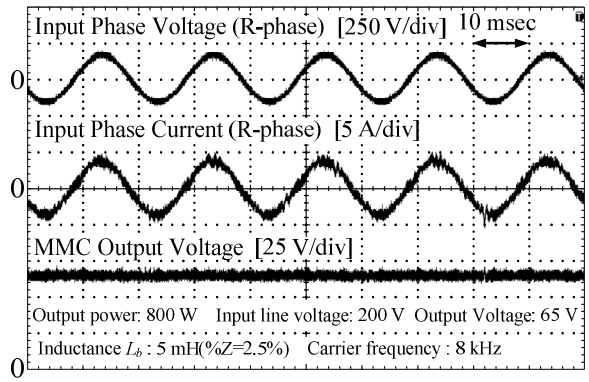

Fig. 5. Waveforms of input voltage, input current and output voltage.

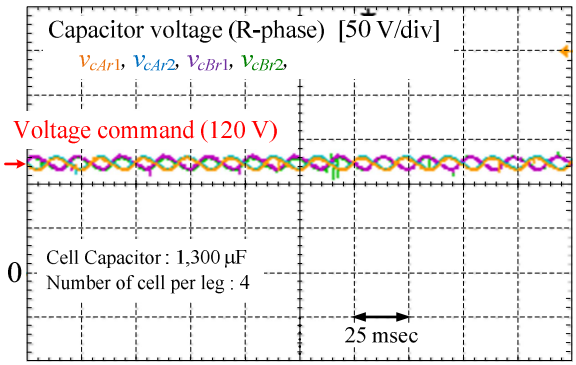

Fig. 6. Waveforms of capacitor voltage in r-phase leg.

VI. Evaluations of overall volume

In this section, the overall volume of the step-down rectifier using the MMC is evaluated. At first, the relationship between the ripple current and the volume of the electrolytic capacitor has been clarified. Specifically, the relationship between the ripple current which affects the lifetime of the electrolytic capacitor and the volume has been considered by the database of commonly-marketed electrolytic capacitors which are generally implemented into many products [5]. At same time, the relationship between the number of cells and the volume of the electrolytic capacitor has been also clarified [5]. Second, as an evaluation for the volume of the heat-sink, the relationship between the input power factor and the total loss of the H-bridge cell is considered in order to design the heat-sink in the worst-case. Finally, the overall volume which includes the volume and the electrolytic capacitor and the volume of the heat-sink is clarified.

6.1. Evaluation of capacitor volume

Figure 7 shows the relationship between the ripple current and the capacitor volume as a database example [6]. The figure in the graph shows the allowable ripple current of one capacitor. Therefore, the number of the capacitors which are connected in parallel on one cell increases with increasing the ripple current. Moreover, the start point of each line means the ripple current and the volume of one capacitor. As a result, the overall volume of the capacitors becomes small by connecting the capacitor with the small allowable ripple current in parallel compared to the utilization of capacitors with the large allowable ripple current. Thus, the parallel connection of capacitors with the small allowable ripple current is better than the utilization of capacitors with the large allowable ripple current in order to achieve the volume reduction of capacitors. Moreover, the ripple current does not change against the capacitance and the number of cells [5]. Thus, the minimum point of capacitor volume against the number of cells achieves the minimum point of the overall volume.

Figure 8 shows the relationship among the number of cells, the overall volume of the capacitor and a withstand voltage ratio. Note that the number of series connection capacitors increases when the required withstand voltage is larger than the withstand voltage of one capacitor. Thus, it is necessary to meet the conditions of the required withstand voltage by series connection of capacitors. Additionally, the required withstand voltage is set 30% more than the value which is calculated by (1). Moreover, the capacitor volume is determined by the multiplied value of the number of series connection capacitors and the number of cells under the same condition for the ripple current. In addition, the withstand voltage ratio is defined as the ratio of the required withstand voltage to the actual withstand voltage when capacitors are connected in series. From Figure 8, the capacitor volume becomes small when the withstand voltage ratio is close to 1.0. On other words, it is possible to achieve the volume minimization by closing the withstand voltage ratio to 1.0. As a conclusion, it is necessary to meet following conditions in order to achieve the volume minimization of the capacitors.

(1) Applying the capacitor with the small ripple current

(2) Maximizing withstand voltage ratio (Approaching to 1.0)

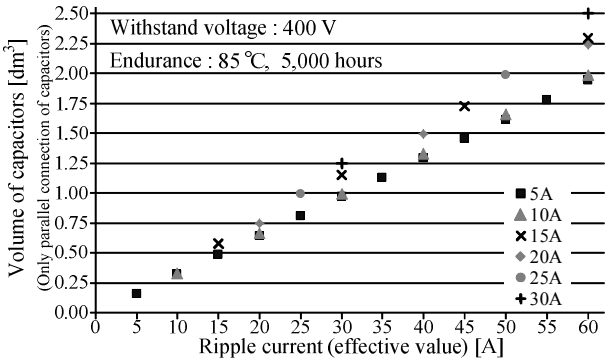

Fig. 7. Relationship between ripple current and capacitor volume.

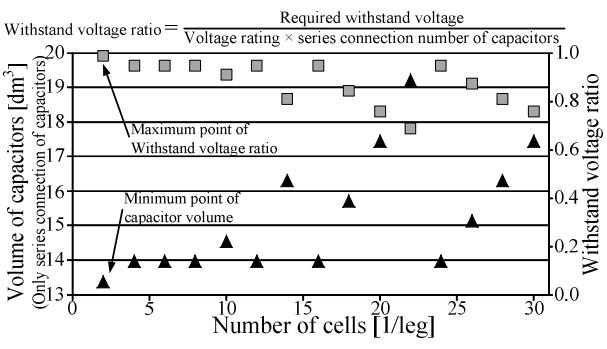

Fig. 8. Relationship between number of cells and capacitor volume.

6.2. Relationship between input power factor and semiconductor losses

The relationship between the input power factor and the total loss of the H-bridge cell is clarified in order to design the heat-sink in the worst-case.

Figure 9 shows the total loss becomes maximum when the input power factor is 1.0. The reason why the total loss increases is to increase the semiconductor loss by the DC component of the arm current. When the input power factor is zero, the semiconductor loss is generated by only the AC component because the input active power (output power) is zero. The semiconductor loss which is generated by the DC component is added gradually because the DC component of the arm current increases as the input power factor is close to 1.0. As a result, it is necessary to design the heat-sink as the worst-case of semiconductor losses when the input power factor is 1.0.

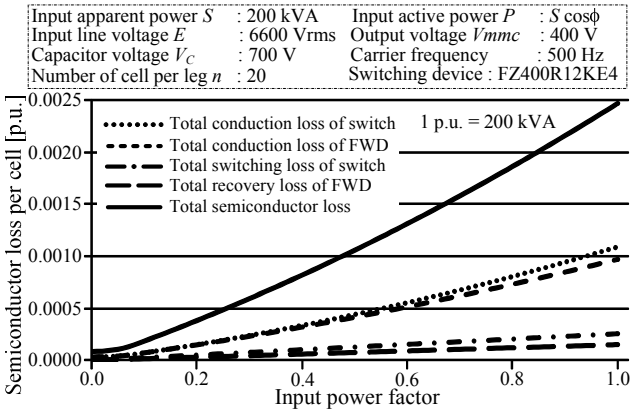

Fig. 9. Relationship between input power factor and semiconductor losses per cell under condition of constant input apparent power

6.3. Conditions for evaluation of overall volume

In the evaluation of the overall volume, the design conditions are set as follows;

(1) The input line voltage is 6.6 kV. The power capacity of the MMC is 200 kVA.
(2) The charge voltage of each capacitor is calculated by (1). Moreover, the required withstand voltage includes 30% margin against the charge voltage.
(3) The capacitor which has the withstand voltage of 400 V and the allowable ripple current of 5 A per one capacitor is applied.
(4) The voltage rating of the switching device is set 80% more than the charge voltage of capacitor. Additionally, the current rating is set twice value as the rated value of the arm current.
(5) The carrier frequency is decided so that the equivalent carrier frequency is 10 kHz.
(6) Loss data in the maximum junction temperature from each datasheet is applied. Moreover, the allowable junction temperature is set 80% of the maximum junction temperature.
(7) The heat-sink is designed based on CSPI [13]. Moreover, CSPI is assumed to 3.0 (Air cooling).
(8) The loss data of SiC-MOSFET is sited from the loss characteristic of one chip [14]-[15]. Thus, the parallel connection number of the chip is decided in order to meet the conditions of the current rating. In addition, the maximum junction temperature is set 175 °C.

6.4. Relationship between input power factor and semiconductor loss

Figure 10 shows the relationship between the volume of one cell and the output voltage of the step-down rectifier using the MMC. The volume of one cell decreases when the output voltage of the MMC increases. The reason why the volume of one cell decreases is to decrease both the parallel connection number of capacitors and semiconductor losses decrease because both the ripple current and the DC component of the arm current decrease.

Figure 11 shows the breakdown of the volume per cell when IGBTs with the voltage rating of 1.7 kV are applied to the H-bridge cell. From Figure 11, the volume of one cell decreases when the output voltage of the MMC increases. Specifically, the volume of capacitors changes significantly compared to the change of the heat-sink volume when the output voltage of the MMC changes. As a result, the

volume of capacitors affects greatly to the volume of the cell compared to the heat-sink volume.

Figure 12 shows the relationship between the overall volume of the MMC and the output voltage of the step-down rectifier using the MMC. The overall volume of the MMC decreases when the output voltage of the MMC increases as with the volume of the cell. From the comparison of Figure 11 and Figure 12, the overall volume does not become minimum under the conditions which the volume of the H-bridge cell becomes minimum. This reason is that the overall volume is changed significantly by the total number of cells even if the volume of the H-bridge cell becomes minimum. Thus, it is difficult to estimate the minimum volume of the MMC from only the volume of the H-bridge cell.

Figure 13 shows the relationship among the number of cell, the overall volume and the withstand voltage ratio when IGBTs with the voltage rating of 1.7 kV are applied to the H-bridge cell. From Figure 13, the change of the heat-sink volume is particularly small compared to the change of the capacitor volume. Therefore, the capacitor volume should be focused when same output voltage of the MMC and the switching device with same voltage rating are applied. Additionally, the relationship between the overall volume and the withstand voltage ratio of capacitors shows that the overall volume becomes small when the withstand voltage ratio is close to 1.0 as with the evaluation of the capacitor volume. Thus, it is necessary to maximize the withstand voltage ratio (approaching to 1.0) in order to obtain the high power density of the step-down rectifier using the MMC.

In conclusion, the conditions in order to obtain the high power density of the step-down rectifier using the MMC are as follows;

(1) Reduction of the step-down ratio of the MMC (The output voltage of the MMC is set to high.)

(2) Design for the number of cell and the series connection number of capacitors in order to maximize the withstand voltage ratio (Approaching to 1.0)

Moreover, the overall volume is calculated in the case which the MMC operates for 10 years when capacitors with the endurance of 5000 hours are applied to the MMC. As a result, the overall volume is 2900 dm^3 based on following conditions; (i) the output voltage of the MMC is 1200 V. (ii) the number of cell is 18. (iii) IGBTs with the voltage rating of 1.7 kV are applied. From this result, the

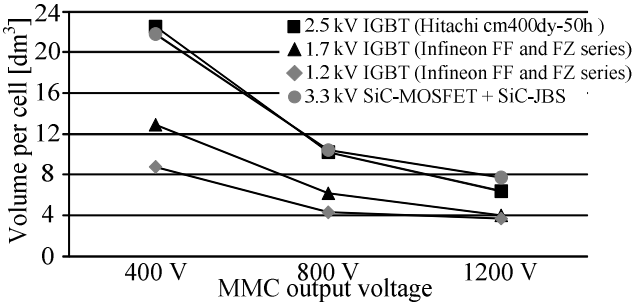

Fig.10. Relationship between output voltage and cell volume.

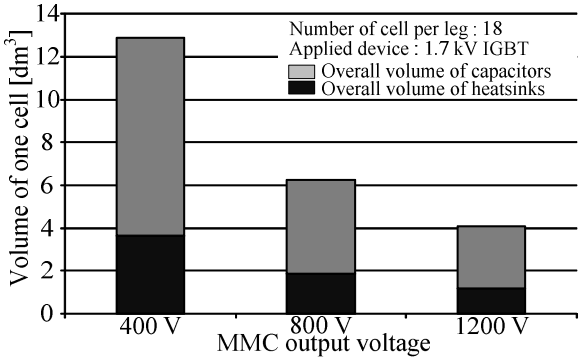

Fig.11. Breakdown of volume per cell

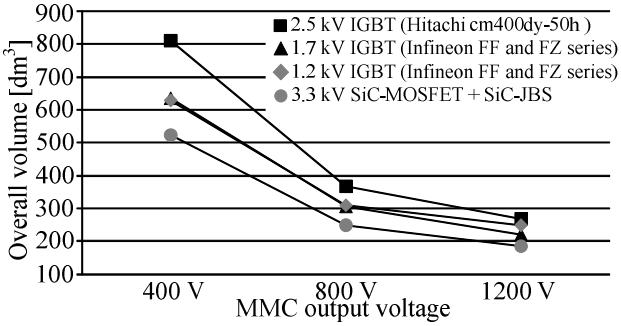

Fig. 12. Relationship between output voltage and overall volume.

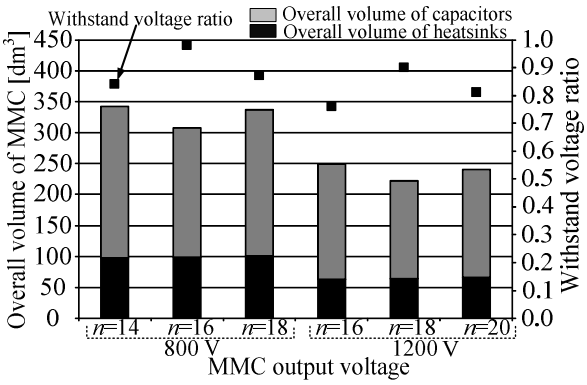

Fig. 13. Relationship among the number of cell, over volume and withstand ratio. (Applying of 1700 V IGBT)

proposed system reduces 80% of the overall volume compared to the conventional power system connected to the utility gird. Thus, the system achieves the volume reduction even considering a reactor volume, a volume of the isolated DC-DC converter and the actual implementation of the MMC.

VII. Conclusions

This paper discussed the volume evaluation of the step-down rectifier using Modular Multilevel Converter (MMC) for the power system connected to the utility gird of 6.6 kV in order to obtain the high power density. Specifically, the clarification of formulas for semiconductor losses, the relationship between the ripple current and the volume of electrolytic capacitors and the relationship between the number of cells per leg and overall volume was detailed.

The conditions in order to obtain the high power density of the MMC are as follows;

- Reduction of the step-down ratio of the MMC (The output voltage of the MMC is set to high.)
  The proposed system reduced approximately 60% of the overall volume in the case which the output voltage increased from 400 V to 1200 V when 1200 V IGBTs are applied.
- Design for the number of cells and the series connection number of capacitors in order to maximize the withstand voltage ratio (approaching to 1.0)
  The proposed system reduced approximately 16% of the capacitor volume in the case which the withstand voltage ratio increased from 0.76 to 0.90.

In conclusion, the proposed system reduced 80% of the overall volume compared with the conventional power system of 200 kVA connected to the utility gird of 6.6 kV.

In future work, the design method in order to minimize the overall volume which is included the reactor volume and the volume of the isolated DC-DC converter will be considered.

References

[1] H. Kakigano, Y. Miura, T. Ise : "Low-Voltage Bipolar-Type DC Microgrid for Super High Quality Distribution", IEEE Trans. on Power Electronics, Vol.25, No.12, pp.3066-3075 (2010)

[2] D. Salomonsson, L. Söder, A. Sannino : "Protection of Low-Voltage DC Microgrids", IEEE Trans. on Power Delivery, Vol.24, No.3, pp.1045-1053 (2010)

[3] M. Glinka, R. Marquardt : "A new ac/ac multilevel converter family", IEEE Trans. Industrial Electronics, vol. 52, No. 3, pp. 662–669, (2005)

[4] N. Thitichaiworakorn, M. Hagiwara, H. Akagi : "Experimental Verification of a Modular Multilevel Cascade Inverter Based on Double-Star Bridge Cells", IEEE Trans. on Industry applications, Vol.50, No.1, pp.509-519 (2014)

[5] T. Nakanishi, J. Itoh : "Capacitor Volume Evaluation based on Ripple Current in Modular Multilevel Converter", 9th International Conference on Power Electronics, No. WeA1-5, (2015)

[6] S. P. Engel, R. W. De Doncker : "Control of the Modular Multi-Level Converter for minimized cell capacitance", EPE2011 (2011)

[7] M. W. Cong, Y. Avenas, M. Miscevic, R. Mitova, J. P. Lavieville, P. Lasserre : "Thermal analysis of a submodule for modular multilevel converters", APEC2014, pp.2675-2681 (2014)

[8] S. Rohner, S. Bernet, M. Hiller, R. Sommer : "Modulation, Losses, and Semiconductor Requirements of Modular Multilevel Converters", IEEE Trans. on Industrial Electronics, Vol.57, No.8, pp.2633-2642 (2010)

[9] T. Modeer, H.P. Nee, S. Norrga : "Loss Comparison of Different Sub-Module Implementations for Modular Multilevel Converter in HVDC Applications", EPE2011 , No. LS2b, (2011)

[10] M Zygmanowski, B. Grzeski, M. Fulczyk R. Nalepa : "Analytical and numerical power loss analysis in Modular Multilevel Converter", IECON2013, Vol. , No., pp.465-470 (2013)

[11] [Online] http://www.nito.co.jp/syohin/syo13.html#items02 (Japanese)

[12] Y. Kashihara, J. Itoh: "Power Losses of Multilevel Converters in Terms of the Number of the Output Voltage Levels", The 2014 International Power Electronics Conference, No. 20A4-4, pp. 1943-1949 (2014)

[13] U. Drofenik, G. Laimer, and J. W. Kolar: "Theoretical Converter Power Density Limits for Forced Convection Cooling", International PCIM Europe Conference, pp.608-619 (2005)

[14] R. Lai, L. Wang, J. Sabate, A, Elasser, and L. Stevanovic, “High-Voltage High-Frequency Inverter using 3.3 kV SiC MOSFETs", Power Electronics and Motion Control Conference (EPE/PEMC), 2012, DS2b.6-1 - DS2b.6-5 (2012)

[15] T. Duong, A. Hefner, K. Hobart, S.H. Ryu, D. Grider, D. Berning, J. M. Ortiz-Rodriguez, E. Imhoff, J. Sherbondy, "Comparison of 4.5 kV SiC JBS and Si PiN Diodes for 4.5 kV Si IGBT Anti-parallel Diode Applications", Applied Power Electronics Conference and Exposition (APEC), pp.1057 - 1063 (2011)